OBJECT-BASED WILDFIRE DAMAGE ASSESSMENT USING PLANETSCOPE IMAGES

Minkyung Chung (1), Yongil Kim (1)

[1] Seoul National University, 1, Gwanak-ro, Gwanak-gu, Seoul, 08826, Korea
Email: mkjung4876@snu.ac.kr; yik@snu.ac.kr

KEY WORDS: Wildfire damage assessment, OBIA, Change detection, PlanetScope

ABSTRACT: Wildfire burn mapping provides information for not only ecological disturbances but also supports post-fire treatment activities. However, due to the labor-intensiveness and high costs of the field-based data collection, remotely sensed satellite images are considered to be efficient alternatives for such tasks. For rapid damage estimation, availability of post-event images becomes a crucial factor, but most of the high-resolution satellite images are captured in long temporal intervals. In this respect, PlanetScope images have considerable potential for applications in disaster management, as Planet provides daily imagery with 3-m spatial resolution from their micro-satellite constellation.

In this study, high-resolution satellite images from PlanetScope were employed to assess the damage from a wildfire, which occurred in the coniferous forest of Gangwon Province, South Korea in April 2019. In doing so, object-based image analysis (OBIA) was performed to reduce the complexity of high-resolution images and computational costs of the subsequent image processing. Image segmentation results were obtained by applying SLIC (Simple Linear Iterative Clustering) and DBSCAN (Density-Based Spatial Clustering of Applications with Noise) utilizing spectral and textural information as object features. The final wildfire burn map was produced from the integration of pixel-based dNDVI (differenced Normalized Difference Vegetation Index) and object boundary. The experimental results were evaluated with manually derived reference data and showed the highest accuracy implying the effectiveness of OBIA when applied in wildfire damage assessment application.

1. INTRODUCTION

As the instant accessibility to wildfire sites is generally limited by its high heat emission, wildfire burn mapping has been widely investigated with remotely sensed images through the literature. Most of the previous studies on wildfire damage assessment using satellite images have been focused on Mediterranean regions or boreal forests (San-Miguel-Ayanz *et al.*, 2009; Chu and Guo, 2014) where massive fires frequently occur yearly. For those large-scale wildfires, moderate to low spatial resolution satellite images are sufficient for discrimination of burned area and monitoring the trend of wildfires over a long period (Levin *et al.*, 2012; Soulard *et al.*, 2016). However, for burned area mapping of local-scale wildfire, higher spatial resolution is required to delineate the details of wildfire-induced damages. Recently, PlanetScope has emerged as a powerful source of high-resolution satellite images. Unlike the conventional high-resolution sensors, which usually capture on-demand images or images with temporal interval of several days, PlanetScope collects high-resolution images from more than 120 Dove satellites on a daily basis, shortening the temporal interval of available images for instant disaster-induced damage assessment. Therefore, in this study, we detected the burned area of a wildfire, which occurred in the coniferous forest of Gangneung, Gangwon Province in South Korea in April 2019 with PlanetScope images.

For change detection, image processing can be divided into pixel-based and object-based, based on the image processing unit. First, pixel-based algorithms are theoretically simple and known to well perform for low and medium-resolution images (Hussain *et al.*, 2013). But in higher resolution images, pixels are not spatially independent, and conventional pixel-based methods become less effective than object-based methods (Aggarwal *et al.*, 2016). Meanwhile, OBIA was introduced to reduce the noises and computational complexity of the subsequent image tasks. However, image segmentation quality may affect the accuracy of the final results, and multiple features should be carefully considered in image segmentation procedures.

The purpose of this study is to enhance the accuracy of burned area detection results with high-resolution satellite images by integrating pixel-based spectral index with the objects from SLIC and DBSCAN. In doing so, additional spectral and textural features were applied to cluster SLIC superpixels and its influence on change detection performance was evaluated with PlanetScope data. To prove the usefulness of employing both spectral and textural features into superpixel clustering, a comparative analysis was performed with the results from spectral features alone.

This paper is organized as follows. Section 2 illustrates the study site and remote sensing data used in this study. Section 3 describes the method to estimate the fire-affected area by integrating pixel-based and object-based image analysis. The experimental results of burned area mapping are presented in Section 4, and the meanings and limitations of the proposed method are addressed as well. As a conclusion, Section 5 sums up the points of the study and

suggests future studies.

2. STUDY SITE AND DATA

2.1 Study Site

The study area is a wildfire site from Gangneung, Gangwon Province in South Korea, which suffered severe wildfire in April 2019 (Figure 1). Gangneung is located in the east side of the Tae Baek Mountains, which is the major mountain ranges in South Korea and features a maritime climate. The fire began on April 4th, 2019 and continued for four days, burning 1,260 ha of pine forests (Gangwon *et al.*, 2019). Considering the fact that Korea Forest Service (2019) defines large forest fires as wildfires burning more 100 ha, 2019 Gangwon wildfire was one of the most severe wildfire cases in nationwide wildfire history.

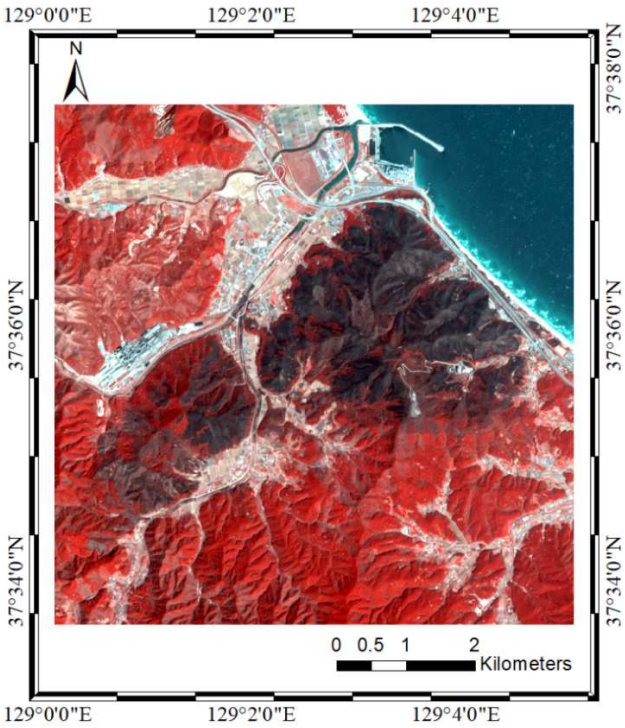

Figure 1. Location of study site
(PlanetScope post-fire image displayed with pseudo colors; R: NIR, G: Green, B: Blue)

2.2 Data

The data used in this study is from PlanetScope satellite, which includes VIS and NIR bands with a spatial resolution of 3m (Table 1 and 2). Pre-fire and post-fire PlanetScope images at level-3B were used in wildfire burn mapping, each captured on April 4 and April 8, 2019 (Figure 2). All the images were obtained as free through Planet Education and Research program (Planet). As PlanetScope images were captured as a continuous strip of the scenes, image mosaicking was performed with edge feathering. Then the mosaicked images were cropped into the area of interest. For PlanetScope level-3B product is an orthorectified scene product with atmospheric (conversion to top of atmosphere reflectance), radiometric (conversion to absolute radiometric values based on calibration coefficients), and geometric (using GCPs and fine DEMs) correction (Planet, 2019), no additional image pre-processing was applied before burned area mapping.

Table 1. Specifications of PlanetScope Level-3B product (Planet, 2019)

Sensor	Spectral Bands	Ground Sample Distance	Radiometric Resolution	Positional Accuracy
PlanetScope	Blue : 455 – 515 nm Green : 500 – 590 nm Red : 590 – 670 nm NIR : 780 – 860 nm	3.7 m (average at reference altitude 475 km)	16 bit (Analytic, radiance)	< 10 m RMSE

Table 2. Specifications of input images used for wildfire damage assessment

Sensor	Acquisition Time (YY/MM/DD)	Description	Pixel Size (Orthorectified)	Image size
PlanetScope	19/04/04	Pre-fire	3 m (Level-3B Product)	2500×2500 (pixels)
	19/04/08	Post-fire		

(a) (b) (c) (d)

Figure 2. PlanetScope subset images used in this study; Pre-fire image captured on April 4, 2019: (a) displayed with true colors (RGB), (b) with pseudo colors (NIR·GB) and post-fire image captured on April 8, 2019: (c) displayed with true colors (RGB), (d) with pseudo colors (NIR·GB) (Includes material © (2019) Planet Labs Netherlands BV. All rights reserved.)

3. METHODOLOGY

The proposed algorithm is devised to enhance the burned area mapping performance with object boundary driven by utilizing spectral and textural information. To obtain the object boundary from the post-fire image, we performed the two-step image segmentation process before change detection; superpixel generation, superpixel clustering. First, for superpixel generation, NIR·GB image was used as an input to SLIC. Then, superpixel clustering using DBSCAN was applied to cluster superpixels into a certain size of objects for change detection based on spatial adjacency with additional color and texture conditions. For burned area detection, NDVI was selected among widely used spectral indices in consideration of available spectral bands from PlanetScope satellite images. Ultimately, the changes were extracted by thresholding pixel-based dNDVI image and recovered to objects using image segmentation results. The following subsections describe the method for estimating the fire-affected area in detail.
Figure 3 shows the overall flowchart of the study.

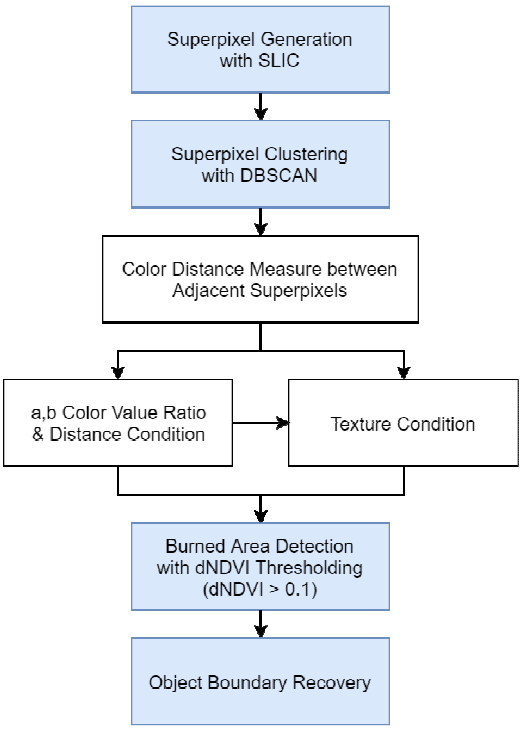

Figure 3. Flowchart of the proposed wildfire burn mapping method

3.1 Superpixel Generation

To segment the post-fire image into objects for burned area detection, firstly image oversegmentation was conducted using SLIC technique, which utilizes color and spatial information of the image to efficiently generate uniform superpixels (Achanta *et al.*, 2010). SLIC is well known for outperforming the previous superpixel methods with high image segmentation quality (Achanta *et al.*, 2012). Moreover, SLIC is advantageous as it requires RGB bands as input and much less input parameter compared with other conventional image segmentation methods. In principle, SLIC performs local clustering in 5-dimensional space defined by L, a, b values from CIELAB color space and x, y pixel coordinates within 2S-by-2S (pixels) search region. As a parameter for the grid interval between initial cluster centers, S means the expected superpixel size from the desired number of superpixels. Considering the size and spatial resolution of the image, the only parameter required for SLIC, S was set as ten thousand, so that the expected size of a single superpixel to be 25-by-25 pixels. However, as shown in Figure 2 (c), it is difficult to visually discriminate the burned area from the surroundings by post-fire RGB image. Therefore, the pseudo-color composite image (NIR·GB image) was used instead of RGB image as an input to SLIC. Such replacement is possible because SLIC operates its clustering based on CIELAB color space which was initially devised as perceptual color space. Thus visually enhanced images could produce improved image segmentation results with proper band combinations.

3.2 Superpixel Clustering

In the following, the previously produced superpixels were clustered into a certain size of objects for efficient change detection. For superpixel clustering, DBSCAN (Ester *et al.*, 1996; Kovesi) was employed to form clusters of superpixels. In doing so, mean Lab color distance between the two adjacent superpixels (Equation 1) was used as a basic clustering distance measure to determine the similarity of superpixels.

$$\text{Lab Color Distance} = \sqrt{(L_1 - L_2)^2 + (a_1 - a_2)^2 + (b_1 - b_2)^2} \tag{1}$$

where L = lightness
a = green–red color components
b = blue–yellow color components in CIELAB color space
(L, a, b with subscript number 1 and 2 correspond to L, a, b values from two adjacent superpixels.)

In addition to Lab color distance, we also used other spectral features, which is a, b color value ratio and distance (Equation 2 and 3), and textural features from co-occurrence metrics of post-fire NDVI images (Figure 4). In CIELAB color space, color is expressed in 3 numerical values, L, a, b, each refers to lightness, green-red and blue-yellow color components. Based on the properties of CIELAB color space, we focused on the fact that even for superpixels that have considerably large Lab color distance, when their colors (hue, to be specific) are similar, it can be included in the same cluster, and they are only appeared to have different lightness because of illumination conditions.

$$\text{a,b Color Value Ratio} = \left|(a_1 / b_1) - (a_2 / b_2)\right| = \text{Differences in Hue} \tag{2}$$

$$\text{a,b Color Distance} = \sqrt{(a_1 - a_2)^2 + (b_1 - b_2)^2} \tag{3}$$

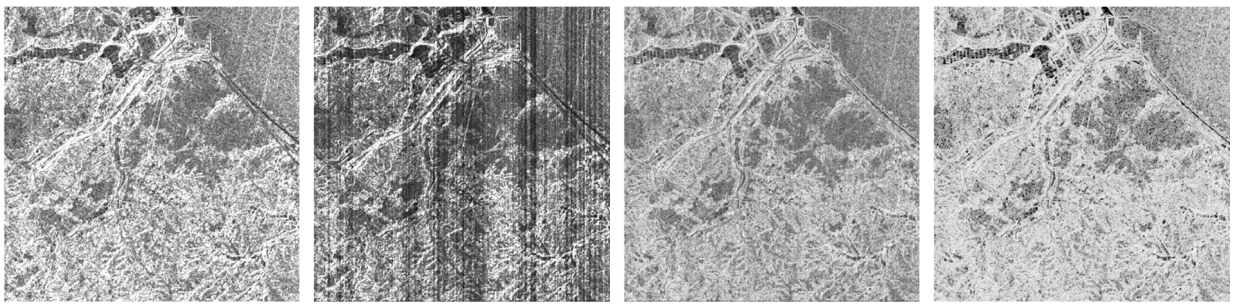

(a) (b) (c) (d)

Figure 4. Co-occurrence metrics from post-fire NDVI image; (a) homogeneity (inversed), (b) dissimilarity, (c) entropy, (d) second moment (inversed)

For estimation of texture similarity, textural features were obtained from post-fire NDVI image, because it shows

clear discrimination between vegetation and non-vegetation, and provides less color-dependent information than RGB images. As measures to determine texture similarity, four co-occurrence metrics (homogeneity, dissimilarity, entropy, and second moment) were selected, which can be easily interpreted and tend to show similar values within the objects. All textures were normalized to values between 0 and 1, and its ratios were measured to evaluate the textural similarity of adjacent superpixels (Equation 4).

$$\text{Texture similarity} = \left(T_1 / T_2\right) \text{ or } \left(T_2 / T_1\right) \leq 1 \text{ for each texture} \quad (4)$$

where T = one of four co-occurrence metrics from NDVI image
(homogeneity, dissimilarity, entropy, second moment)
(T with subscript number 1 and 2 correspond to texture values from two adjacent superpixels)

All the features used to cluster superpixels were calculated from mean color and texture values of pixels within each superpixel, and these features were organized as stepwise conditions to determine whether the neighboring superpixels can be clustered into a single object or not.
As shown in Figure 5, fundamentally, DBSCAN is performed for each superpixel, one-by-one, finding neighboring superpixels and comparing the clustering distance measure with certain threshold distance (E_C). If some neighboring superpixels satisfy the conditions, find their neighboring superpixels again and repeat the clustering procedures until there are no more neighboring superpixels to be clustered. Then, it moves to the next superpixel to form a new cluster unless it is already grouped into previously-made superpixel clusters. Because the accuracy of texture information is known to be low when used without spectral information, spectral conditions were applied first. Then, under the assumption that spectral similarities are guaranteed to some extent, texture conditions were applied as ancillary data rather than primary data. All the coefficients included in Figure 5 (decision tree diagram for superpixel clustering) were determined by trial-and-error from our previous studies on urban change detection (Chung *et al.*, 2019), extended to disaster damage assessment.

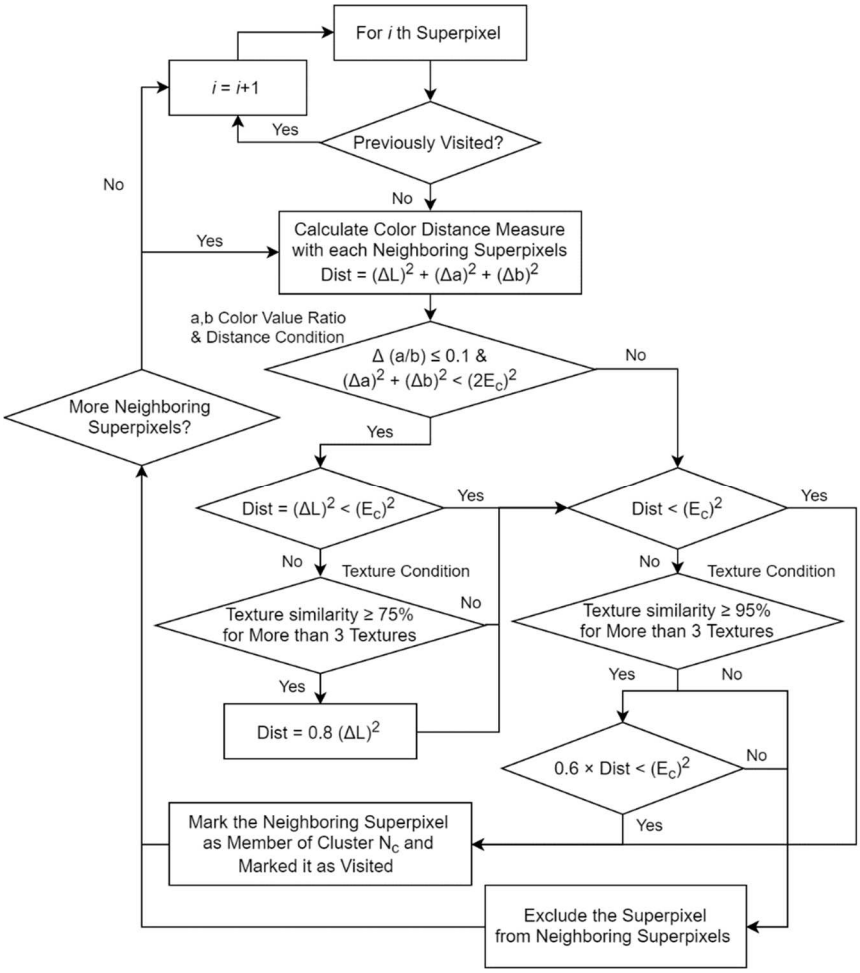

Figure 5. Decision tree diagram for superpixel clustering using both color and texture similarity

3.3 Burned Area Detection and Object Boundary Recovery

The burned area was detected by differenced NDVI (Equation 5 and 6), considering the available spectral bands from PlanetScope images. By employing the vegetation index to determine the fire-affected area, the main change intended to detect in this study was limited to the wildfire-induced vegetation loss. The dNDVI values were calculated pixel-wise using pre-fire and post-fire images. It is due to the possibility that object features may not reflect the overall trend of features within the object when obtained by simply averaging individual values. Therefore, the pixel-based dNDVI image was used instead, and non-vegetation masking was applied to exclude the area that has NDVI values less than zero from the pre-fire image. Then, the pixels with dNDVI values higher than 0.1 were extracted as regions with the high possibility of being affected by the wildfire.

$$\mathrm{NDVI} = \frac{\mathrm{NIR} - \mathrm{Red}}{\mathrm{NIR} + \mathrm{Red}} \tag{5}$$

$$\mathrm{dNDVI} = \mathrm{NDVI}_{\mathrm{pre-fire}} - \mathrm{NDVI}_{\mathrm{post-fire}} \tag{6}$$

As the extracted change candidates from dNDVI thresholding appear to have noises, object boundary recovery was performed based on the final image segmentation results. To recover the object boundary of the post-fire image, we considered the whole single object as changed regions, when more than 50% of the pixels from an object are included in the changed regions. Finally, the ultimate change detection results were produced and evaluated with reference data visually and quantitatively.

4. EXPERIMENTAL RESULTS

The point of this study is to verify the influence of employing both spectral and textural information in image segmentation of high-resolution images, and further, in change detection performance. The proposed wildfire change detection method was applied to PlanetScope high-resolution satellite images. In doing so, pixel-based dNDVI values were used as a measure to detect the burned area and integrated with the objects generated from SLIC and DBSCAN, which utilizes several object features for clustering. The final burned area mapping results were compared with manually-driven reference data for evaluation of change detection performance.
However, due to the difficulties in obtaining the segmentation reference for high-resolution satellite images, the evaluation for image segmentation quality was replaced with qualitative analysis. Through visual inspection (Figure 6), we found that textural information can improve the segmentation quality when integrated with proper spectral features. It is also clearly shown in the stepwise images that the conditions applied in the process of superpixel clustering gradually clustered the superpixels with similar color and texture features while maintaining the boundaries with other covers.

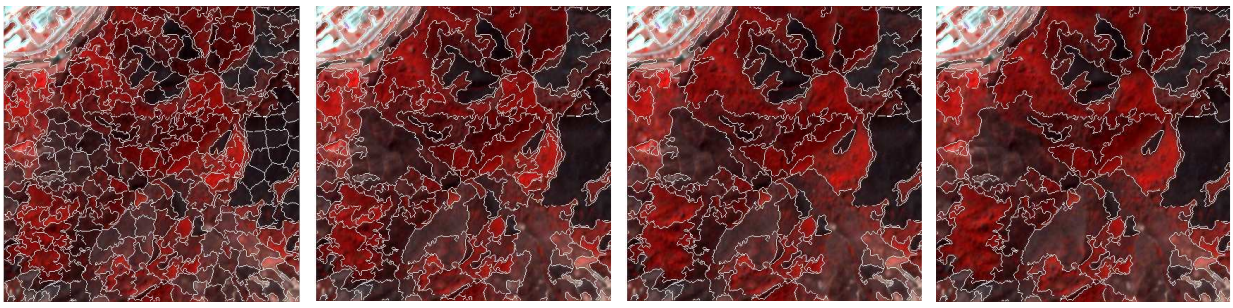

(a) (b) (c) (d)

Figure 6. Zoom image for visual inspection of image segmentation results from (a) SLIC superpixels, (b) DBSCAN with only Lab color distance, (d) DBSCAN with additional color conditions, (e) DBSCAN with both color and texture conditions

Moreover, the burned area mapping results from the proposed method (Figure 7) showed similar trends with reference data, especially, even well representing the boundaries of the narrow road located on the mountainside. But the results still contain some falsely detected changes, which are considered to be induced by the temporal interval between post-fire images used in detecting burned area and generating reference, each captured on April 8 and April 20, 2019. In other words, the regions with low spectral responses from the earlier image were misjudged as burned area, but seasonal changes after the wildfire improved the discriminating power between burned and unburned regions.

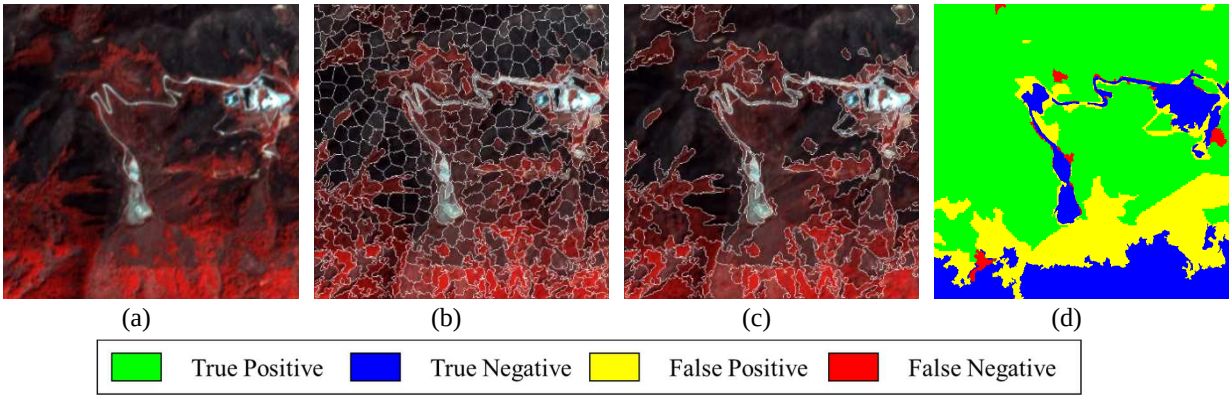

Figure 7. Zoom image for visual inspection (a) post-fire image, (b) image segmentation results from SLIC superpixel, (c) image segmentation results from DBSCAN with both color and texture conditions, (d) burned area detection results from the proposed method, compared with reference data

To prove the influence of integrating the spectral and textural conditions in superpixel clustering and its effects on object-based image analysis, change detection was also performed for stepwise conditions composing the proposed method. The accuracy of change detection was assessed for five methods, including the proposed method with reference data (Table 3 and 4). Among the comparison group, the proposed method showed the highest accuracy for both producer's and user's accuracy with the highest kappa coefficient. Thus it clearly showed the advantages of handling high-resolution satellite images in object unit and potential for further improvement when additional features are applied properly.

Table 3. Accuracy assessment (Overall accuracy, producer's accuracy, and user's accuracy)

Method	Overall accuracy (%)	Producer's accuracy (%)		User's accuracy (%)	
		Unburned	Burned	Unburned	Burned
Pixel-based	96.427	98.978	86.926	96.575	95.805
Superpixel-based	96.434	99.252	86.204	96.312	96.945
Object-based (with only Lab color distance)	96.307	99.241	85.729	96.165	96.905
Object-based (with additional color conditions)	96.609	99.081	87.394	96.701	96.226
Proposed object-based (with both color and texture conditions)	96.713	99.193	87.506	96.718	96.689

Table 4. Accuracy assessment (Commission error, omission error, and Kappa coefficient)

Method	Commission error (%)		Omission error (%)		Kappa coefficient
	Unburned	Burned	Unburned	Burned	
Pixel-based	1.022	13.074	3.425	4.195	0.8892
Superpixel-based	0.748	13.796	3.688	3.055	0.8903
Object-based (with only Lab color distance)	0.759	14.271	3.835	3.095	0.8866
Object-based (with additional color conditions)	0.919	12.606	3.299	3.774	0.8948
Proposed object-based (with both color and texture conditions)	0.807	12.494	3.282	3.311	0.8982

5. CONCLUSION

For the accurate delineation of the burned area boundary, the proposed method integrated pixel-based dNDVI and object boundary from SLIC and DBSCAN. To cluster the SLIC superpixels, DBSCAN organized the sequential conditions considering not only Lab color distance but also additional spectral and textural information. Textural information used in this study was obtained from co-occurrence metrics of post-fire NDVI images, as it provides discriminative responses for vegetation and non-vegetation with less color-dependent properties. The burned area was detected by thresholding the pixel-based dNDVI image to preserve the details of pixel-wise responses from the vegetation. Then, the previously generated object boundary was used to recover the objects from the pixel-

wise change candidates. The final change detection results were compared with the results from stepwise conditions composing the proposed method. From the visual inspection and accuracy assessment, the proposed method showed the highest change detection accuracy with the highest Kappa coefficient while well preserving the details of the burned area. The experimental results validate the significance of applying multiple spectral and textural conditions in image segmentation but organized in a proper way. Besides, as the PlanetScope images are provided with acceptable product quality on a daily basis, it has considerable potential for disaster management applications. In the future studies, further investigation on the data interoperability of PlanetScope will enable the temporal intervals for disaster damage assessment to be even shortened.

ACKOWLEDGEMENTS

This research was supported by a grant (2019-MOIS32-015) of Disaster-Safety Industry Promotion Program funded by Ministry of Interior and Safety (MOIS, Korea).

REFERENCES

Achanta, R., Shaji, A., Smith, K., Lucchi, A., Fua, P., Süsstrunk, S., 2010. SLIC Superpixels. EPFL Technical Report 149300.

Achanta, R., Shaji, A., Smith, K., Lucchi, A., Fua, P., Süsstrunk, S., 2012. SLIC superpixels compared to state-of-the-art superpixel methods. IEEE Transactions on Pattern Analysis and Machine Intelligence, 34(11), pp. 2274-2282.

Aggarwal, N., Srivastava, M., Dutta, M., 2016. Comparative analysis of pixel-based and object-based classification of high resolution remote sensing images—a review. International Journal of Engineering Trends and Technology, 38(1), pp. 5-11.

Chu, T., Guo, X. 2014. Remote sensing techniques in monitoring post-fire effects and patterns of forest recovery in boreal forest regions: A review. Remote Sensing, 6(1), pp. 470-520.

Chung, M., Han, Y., Kim, Y., 2019, Object-based change detection with textural information in high-resolution satellite images, In: International Symposium on Remote Sensing, 17-19 April, 2019, Taipei, Taiwan.

Ester, M., Kriegel, H. P., Sander, J., Xu, X., 1996. A density-based algorithm for discovering clusters in large spatial databases with noise. In: International Conference on Knowledge Discovery and Data Mining (KDD-96), 2-4 August, 1996, Portland, Oregon, USA, 96(34), pp. 226-231.

Gangwon, Research Intstitute for Gangwon, Gangwon KOFST (Korean Federation of Science & Technology Societies, 2019. 1st Gangwon Province Disaster Prevention (Wildfire) Forum 2019. Retrieved August 30, 2019, from http://pms.rig.re.kr/RPMS/Resource/AttachDownHP.ashx?PARAM=QQBBADAAMAAwADAAMAAwADUAOAAxADMAJgAxAA==/

Hussain, M., Chen, D., Cheng, A., Wei, H., Stanley, D., 2013. Change detection from remotely sensed images: From pixel-based to object-based approaches. ISPRS Journal of Photogrammetry and Remote Sensing, 80, pp. 91-106.

Korea Forest Service, 2019. Comprehensive Plan for the Prevention of National Forest Fire 2019. Retrieved August 30, 2019, from http://www.forest.go.kr/kfsweb/cop/bbs/selectBoardArticle.do?bbsId=BBSMSTR_1008&mn=NKFS_06_09_05&nttId=3127725/

Kovesi P., MATLAB and Octave Functions for Computer Vision and Image Processing. Retrieved August 30, 2019, from http://www.peterkovesi.com/matlabfns/

Levin, N., Heimowitz, A. 2012. Mapping spatial and temporal patterns of Mediterranean wildfires from MODIS. Remote Sensing of Environment, 126, pp. 12-26.

Planet, 2019. Planet Imagery Product Specifications, Retrieved August 30, 2019, from https://assets.planet.com/docs/combined-imagery-product-spec-final-may-2019.pdf.

Planet, Planet Education and Research Program, Retrieved August 30, 2019, from https://www.planet.com/markets/education-and-research/

San-Miguel-Ayanz, J., Pereira, J. M., Boca, R., Strobl, P., Kucera, J., Pekkarinen, A. 2009. Forest fires in the European Mediterranean region: mapping and analysis of burned areas. In Earth observation of wildland fires in Mediterranean ecosystems. In: Earth observation of wildland fires in Mediterranean ecosystems, edited by Chuvieco E., Springer, Berlin, pp. 189-203.

Soulard, C., Albano, C., Villarreal, M., Walker, J. 2016. Continuous 1985–2012 Landsat monitoring to assess fire effects on meadows in Yosemite National Park, California. Remote Sensing, 8(5), 371.